

# EXPERIMENTAL CHARACTERIZATION OF SEEDED FEL AMPLIFIER AT THE NSLS SDL

T. Watanabe<sup>#</sup>, D. Liu, J.B. Murphy, J. Rose, T. Shaftan, T. Tsang, X.J. Wang, and L.H. Yu,  
 NSLS, BNL, Upton, NY 11973, U.S.A.  
 P. Sprangle, NRL, Washington D.C. 20375, U.S.A.

## Abstract

Experimental characterization of a near-IR FEL amplifier at the NSLS SDL is presented in this report. SASE was observed from 0.8-1  $\mu\text{m}$  with 5 orders of magnitude gain. We have experimentally demonstrated saturation of a laser seeded FEL amplifier and control of the FEL output by the seed laser. Nonlinear harmonics have also been explored. The FEL pulse length for the first three harmonics was experimentally characterized and the increase of the FEL pulse length with harmonic number was observed for the first time. Computer simulation confirmed that the observed wide spectrum of the laser seeded FEL is due to the positive chirp of the seed laser.

## INTRODUCTION

Recent success with single pass FEL amplifiers [1-4] and energy recovery linacs [5] has made it feasible to explore using laser seeded FEL amplifiers for directed energy applications [6-7]. For directed energy applications [7] a MW-class FEL at near-IR wavelengths is required. Major challenges to realizing a MW-class laser seeded FEL are high-brightness electron beams and FEL amplifier performance. An experimental program was initialized at the NSLS Source Development Laboratory (SDL) to demonstrate the critical FEL amplifier technologies for high average power applications; especially to investigate various schemes of improving the FEL efficiency and controlling of the FEL output radiation using pinched e-beam technique [7].

The SDL is an ideal platform to study laser seeded FEL amplifiers. We have successfully achieved high gain harmonic generation (HG) saturation at 266 nm with an 800 nm seed [4]. The main components of the SDL FEL are a high-brightness electron accelerator, HG FEL, together with sophisticated electron and photon beam instrumentation. The accelerator system of the SDL consists of a 1.6 cell BNL photo-injector driven by a Ti:Sapphire laser system and a five section 2856 MHz SLAC type traveling wave linac capable of producing a 250 MeV electron beam. The magnetic chicane bunch compressor at the SDL produces sub picosecond (ps) long electron bunches with a peak current of a few hundred amperes. The high brightness electron beam transits the 10 meter long NISUS undulator for single pass FEL amplifier operation.

After a brief discussion of the SDL experimental setup we will present the experimental characterization of SASE operation at 0.8-1  $\mu\text{m}$  and also a laser seeded FEL amplifier at 0.8  $\mu\text{m}$ . The laser seeded FEL energy and spectrum along the undulator were measured. Both the transverse and longitudinal distribution of the fundamental and harmonic radiation of the FEL was experimentally characterized. The wide spectrum observed for the laser seeded FEL was confirmed by computer simulation to be caused by a positive chirp of the seed laser.

Table 1: NISUS and electron beam parameters

$\lambda_u(\text{cm})$	3.89	E (MeV)	102
$K_u$	1.1	$\tau_{\text{FWHM}}$ (ps)	1.5
$L_u$ (m)	10	I (A)	300
$\lambda_r(\mu\text{m})$	0.8 to 1.0	$\tau_{\text{laser}}$ (ps)	4.5

## EXPERIMENTAL SETUP

The laser seeded FEL uses an experiment setup similar to that used for HG [4] but with some modifications, such as new seeding optics and diagnostics for 0.8-1  $\mu\text{m}$ . One of the unique features of the SDL laser system is that it was designed in such way that a single laser system is used to drive both the photocathode RF gun and to provide a seed laser pulse. This setup make it possible to achieve sub-ps timing jitter between the seed laser and the electron beam. Table 1 lists the undulator, seed laser and electron beam parameters used for the laser seeded FEL experiment. For the seeded FEL experiment only the radiator of the HG system (10 m NISUS) was used. The new matching optics for the seed laser focuses the seed laser into the NISUS undulator instead of the HG modulator. There are 16 three-position beam profile monitors (BPM) distributed along NISUS and they have been used for both e-beam and seed laser profiles and alignment. One of the three positions of the BPM is just inserting a mirror into the beam path which is primarily used for FEL radiation diagnostics.

There is a dipole magnet after the NISUS undulator which bends the electron beam to the beam dump. The beam profile monitor in front of the beam dump was used to monitor the electron beam energy and energy modulation. The FEL radiation can also be transported by a periscope to the diagnostic station for characterization. The diagnostics station allows us to fully characterize the FEL output. The measurement instruments include a 10 GHz photodiode, a Joule-meter, spectrometers, a CCD camera, a commercial Frequency-Resolved Optical Gating device (FROG) and a femtosecond streak camera.

\* Work supported by Office of Naval Research.

<sup>#</sup> twatanabe@bnl.gov

The major steps of the experiment are electron beam and trajectory optimization, seed laser and e-beam synchronization, and FEL output characterization. SASE radiation was used to optimize the electron beam and the trajectory inside the NISUS undulator. Synchronization of the picosecond seed laser and the electron beam was realized in two steps. In the first step, the seed laser and SASE were observed using the 10 GHz diode and 6 GHz fast scope; the seed laser delay line is adjusted to bring the e-beam and seed laser to within 50 ps. Final synchronization was achieved by observing the electron beam energy modulation while adjusting the seed laser delay. FEL properties are measured at the exit of the undulator. To study the FEL evolution along the undulator the electron beam was steered off the forward trajectory with steering magnets distributed along the undulator.

### SEEDED FEL CHARACTERIZATION AT SATURATION

The experimental characterization of the SASE and laser seeded FEL at saturation is presented in this section. The evolution of the seeded FEL spectrum along the undulator was measured. Both the transverse and longitudinal profiles of the laser seeded FEL fundamental and harmonics were characterized.

#### SASE Observation

SASE was used not only to optimize the electron beam and its trajectory inside the NISUS undulator but also to adjust the electron beam energy so the seed laser will be in resonance. Figure 1 shows the SASE spectrum from 0.8 to 1  $\mu\text{m}$ .

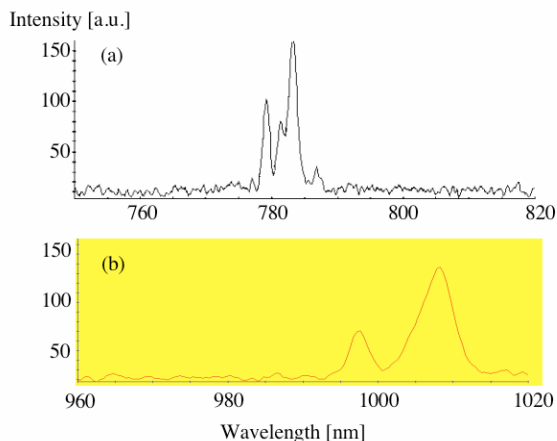


Figure 1: Spectra of SASE at (a) 785 nm and (b) 1.0  $\mu\text{m}$ .

#### FEL Gain and Saturation Observation

The FEL gain and saturation were characterized as we steered the electron beam off the forward trajectory inside NISUS. Figure 2 shows the maximum FEL energy measured at the diagnostic station using a Joule meter (Molelectron J3S-10) as the beam is steered off along the undulator. We optimized the FEL gain as the seed laser power was decreased. It can clearly be seen that saturation

of the FEL is achieved since the FEL gain deviates from exponential behavior. For the purpose of comparison, we also plotted the SASE growth on the Fig. 2. Another point we would like to make is that the seed laser spot size is about a factor of three larger than the electron beam so the seed laser energy is about one order of magnitude over estimated. In summary, we have demonstrated saturation of a seeded FEL and observed more than three orders of FEL gain over the input seed laser.

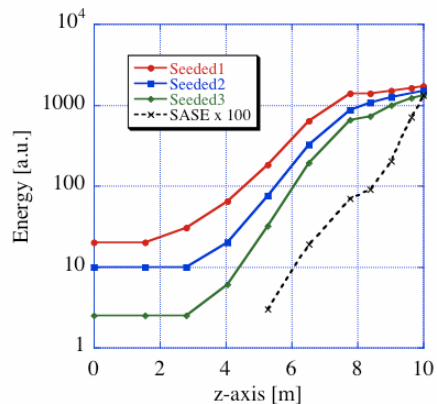


Figure 2: FEL energy vs distance along the undulator  $z$ .

#### Transverse Profiles

When the seeded FEL reaches saturation significant harmonic radiation is expected due to nonlinear harmonic generation, especially for FEL operation at near-IR wavelengths. Energies at the first three harmonic were measured in earlier experiments [2], but the transverse profiles for those harmonic were never characterized. Transverse distributions of the fundamental FEL radiation and the harmonics are important for directed energy applications since they could cause damage to the guiding optics. Figure 3 shows the FEL harmonic profiles at the end of the NISUS undulator. We would like to point out that narrow band pass filters (10 nm) were installed before the CCD camera for each harmonic measurement. The fundamental and second harmonic was obtained with the same CCD camera while the third harmonic was obtained using a different CCD camera due to the need for UV optics.

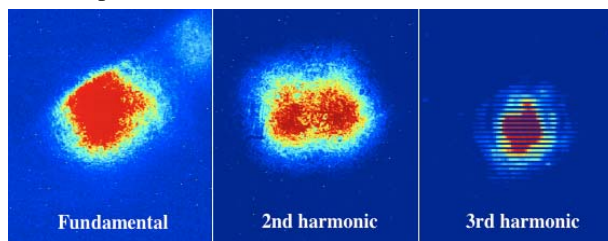


Figure 3: Fundamental and harmonic FEL profiles.

#### FEL Pulse Length Characterization

One of the areas in single pass FEL R&D that can be explored is the evolution of the FEL pulse length. Since the seeded pulse length used in this experiment is longer than that of the electron beam, it is expected that the FEL pulse length is determined by the e-beam.

But other effects such as the slippage of the FEL pulse relative to the electron beam could lead to FEL pulse lengthening. We have also successfully demonstrated superradiance and nonlinear evolution of a femto-second seeded FEL [8].

To study the longitudinal distribution of fundamental FEL radiation and harmonics, a streak camera (Hamamatsu Photonics, C6860) with reflective optics was employed. The resolution of the streak camera was determined to be 700 fs (FWHM) using a 100 fs Ti:Sap. laser oscillator. The FEL light was transported to the streak camera with reflective optics only. For each harmonic measurement a narrow bandpass filter (10 nm) was placed in front of the streak camera.

The pulse length of the SASE radiation and the laser seeded radiation, including the second and third harmonics, is shown in Figure 4. The average pulse length (FWHM) for the fundamental is 1.6 ps, that of the 2nd harmonic was 1.8 and that of 3rd was 2.4 ps. The average pulse length for the SASE light was 1.5 ps. One of the surprises of this study is that the pulse lengthening was observed instead of the shortening as predicted by theory. We will discuss a possible explanation in the next section.

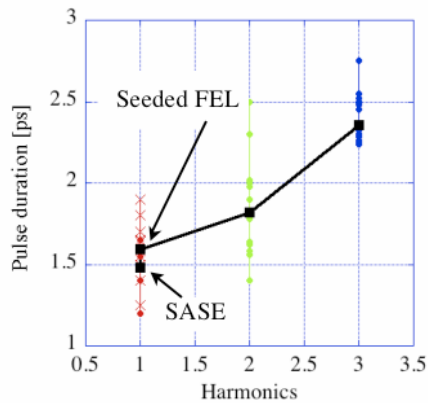


Figure 4: Fundamental and harmonic FEL pulse length.

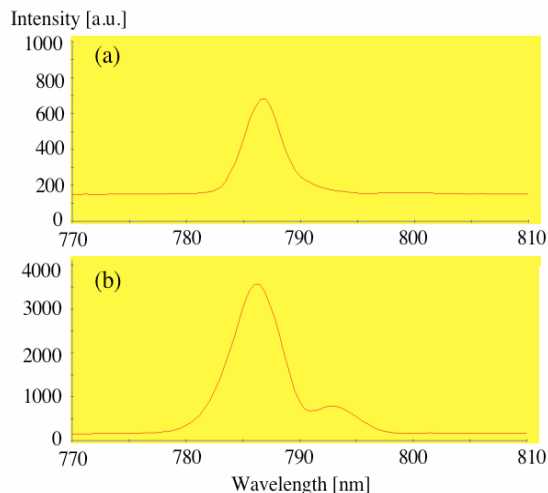


Figure 5: Spectra of seeded FEL at the (a) middle and (b) end of the NISUS undulator.

## FEL Spectrum Evolution

Compared to a SASE FEL, the laser seeded FEL output will be fully coherent and the central wavelength will be determined by the seed laser. We measured the FEL spectrum evolution along the undulator by the steering the e-beam off the forward trajectory along the undulator. We observed a single lobed spectrum until saturation was reached (Figure 5). The spectrum width was found to be constant and wide (4.5 nm). The seed laser spectrum is about 7 nm wide. We will discuss the reason for the wide spectrum of laser seeded FEL; we believe we have for the first time observed a chirp of the FEL output due to a seed laser chirp, but no chirp of the electron beam.

## DISCUSSION AND CONCLUSION

The experimental characterization of the SASE and laser seeded FEL at near-IR wavelengths was presented in this report. We observed SASE from 0.8-1  $\mu\text{m}$  with five orders of magnitude gain. We have demonstrated saturation of the laser seeded FEL. We presented experimental characterization of the spectrum and also the transverse and longitudinal distributions of the laser seeded FEL at saturation.

To understand the wide FEL spectrum observed we carried out simulation studies using the 3-D computer code GENESIS1.3 [9]. Using the seed laser and electron beam parameters listed in Table 1 we simulated the FEL output for a seed laser with i.) no chirp, ii) a positive chirp and iii.) a negative chirp. For all cases, no electron beam energy chirp is used. GENESIS1.3 predicts a positive chirped FEL output even without any chirp on the electron beam and the seed laser. Similar behavior was observed for a SASE FEL [10-11]. Furthermore, simulation shows that the FEL chirp can be controlled by the seed laser and a wide spectrum (3.5 nm) is expected when the seed laser is positive chirped. When the spectrum resolution is taken into consideration (0.5 nm) the simulation agrees with our experimental observation. Control of the FEL chirp could be explored for a cascaded HGHG FEL to produce ultra-short FEL pulses since the seed laser chirp is relative easy to implement without any electron beam chirp. Table 2 summarizes the FEL spectrum width for different seed laser chirps.

The unexpected observation of the FEL pulse length increase with harmonic number will be further investigated in the future. Here we consider a brief examination of the possible explanations. It is well known that the time resolution of a streak camera depends on the wavelength of the incident light since the energy spread of the photoelectrons becomes larger as the wavelength becomes shorter. The time spread,  $\delta T$ , can be evaluated by [12],

$$\delta T = 1.4 \left( \frac{m}{2e} \right) \frac{(\delta E)^{1/2}}{E}, \quad (1)$$

where  $m$  is the rest mass of an electron,  $e$  is the electric charge,  $\delta E$  is the energy spread of photoelectrons and  $E$  is the accelerating field near the photocathode surface.

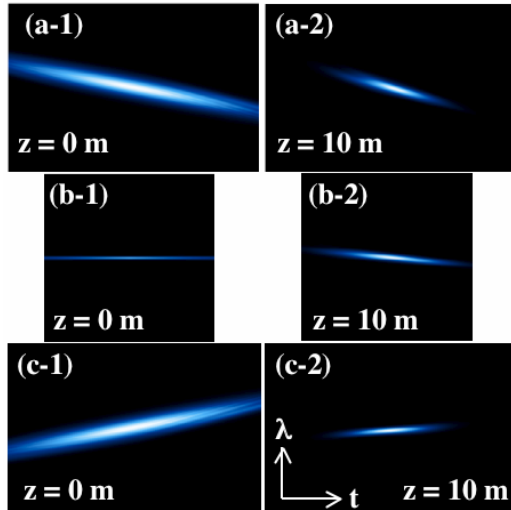


Figure 6: Longitudinal phase space distributions of FEL calculated by GENESIS1.3. (a) positive chirp input (b) no chirp input and (c) negative chirp input. Left pictures are input and right are output. Horizontal axis is time and vertical is wavelength.

Table 2: Output FEL bandwidth vs chirp of seed laser

Input chirp	Negative	None	Positive
Bandwidth (nm)	1.5	2.0	3.5

The time spread  $\delta T$  has also been estimated by Hamamatsu Photonics to be 796 fs for 400 nm and 944 fs for 250 nm. We conclude that our experimental results are not limited by the streak camera resolution. Another possible explanation is that the theory for FEL harmonics is valid only in the linear regime (exponential gain) or near the saturation. In our case the FEL has reached deep saturation and the long electron beam tail, plus slippage

could lead to the increase of the FEL pulse length with harmonic number.

In the future, we will explore various techniques to improve the FEL amplifier efficiency and performance such as kilo-ampere electron beam generation, optical guiding of the FEL, detuning and the use of a strong focusing undulator.

We are grateful for support from the NSLS and BNL director's office and this work is supported by the Office of Naval Research and U.S. Department of Energy under contract No. DE-AC02-98CH1-886. References

## REFERENCES

- [1] S. Milton, *et al.*, *Science* **292**, 2037 (2001).
- [2] A. Tremaine, *et al.*, *Phys. Rev. Lett.* **88**, 204801-1 (2002).
- [3] V. Ayvazyan, *et al.*, *Phys. Rev. Lett.* **88**, 104802-1(2002).
- [4] L.H. Yu, *et al*, *Phys. Rev. Lett.* **91**, 074801-1 (2003).
- [5] G. Neil, *et al*, *Phys. Rev. Lett.* **84**, 662 (2000).
- [6] D.C. Nguyen and H.P. Freund, *NIM A***507**, 120 (2003).
- [7] P. Sprangle, *et al*, *IEEE J. Quantum Electronics*, **40** 1739 (2004).
- [8] T. Watanabe *et al*, THPP032, this proceeding.
- [9] S. Reiche, *NIM A***429**, p. 243 (1999).
- [10] S. Krinsky and Z. Huang, SLAC-PUB-9633, Jan. 2003.
- [11] Z. Huang and S. Krinsky, SLAC-PUB\_10310, Jan. 2004.
- [12] T. Tsuchiya, Study on Ultrahigh Speed Streak Camera (Hamamatsu Photonics, 1985), in Japanese.